

Contribution of human melanopsin retinal ganglion cells to steady-state pupil responses

Sei-ichi Tsujimura¹, Kazuhiko Ukai², Daisuke Ohama¹, Atsuo Nuruki¹ & Kazutomo Yunokuchi¹

¹*Department of Information Science and Biomedical Engineering, Kagoshima University, Kagoshima, JAPAN*

²*Department of Applied Physics, School of Advanced Science and Engineering, Waseda University, Tokyo, JAPAN*

Abstract

The recent discovery of melanopsin-containing retinal ganglion cells (mRGCs) has led to a fundamental reassessment of non-image forming processing, such as circadian photoentrainment and the pupillary light reflex. In the conventional view of retinal physiology, rods and cones were assumed to be the only photoreceptors in the eye and were, therefore, considered responsible for non-image processing. However, signals from mRGCs contribute to this non-image forming processing along with cone-mediated luminance signals; although both signals contribute, it is unclear how these signals are summed. We designed and built a novel multi-primary stimulation system to stimulate mRGCs independently of other photoreceptors using a silent-substitution technique within a bright steady background. The system allows direct measurements of pupillary functions for mRGCs and cones. We observed a significant change in steady-state pupil diameter when we varied the excitation of mRGC alone, with no change in luminance and color. Furthermore, the change in pupil diameter induced by mRGCs was larger than that induced by a variation in luminance alone: that is, for a bright steady background, the

mRGC signals contribute to the pupillary pathway by a factor of three times more than the L- and M-cone signals.

Introduction

The non-image forming processing centers in the brain receive brightness information not only from the novel melanopsin-containing retinal ganglion cells (mRGCs) but also from classical photoreceptors, rod and cones (Ruby et al, 2002; Panda et al, 2002; Lucas et al, 2003; Mrosovsky & Hattar, 2003; Hattar et al, 2003; Panda et al, 2003) although it is still unclear how signals from the classical photoreceptors and mRGCs are summed and contribute to non-image forming pathways. In a study using transgenic animals, Lucas *et al.* measured pupil light reflex as a function of irradiance (Lucas et al, 2003) and showed that signals from classical photoreceptors contribute to the pupillary control mechanism primarily under conditions of low irradiance, whereas melanopsin was required for full pupil constriction at high irradiance. In humans it is difficult to investigate how signals from the classical photoreceptors and mRGCs are summed and contribute to non-image forming pathways. The challenge stems primarily from the need to isolate each photoreceptor type. To isolate mRGCs previous reports have used experimental situations where functional rods and cones are absent, for example, in blind human subjects (Zaidi et al, 2007), in transgenic animals lacking rods and cones (e.g, Lucas et al, 2001; Panda et al, 2002; Ruby et al, 2002; Lucas et al, 2003) and by pharmacological blockade of rods and cones in monkey (Gamlin et al, 2007). Although these studies have demonstrated that mRGCs contribute to the pupil responses the extent of their relative contribution is difficult to assess in the absence of cones. Measurement of sustained pupil responses (Gamlin et al, 2007; Young & Kimura, 2008; Kardon et al, 2009) or the use of long-duration test stimuli (McDougal & Gamlin, 2010) are alternative approaches to achieving isolation of mRGCs but these are based

on the assumption that the sensitivity of mRGCs is higher than cones at low temporal frequencies. For example, McDougal & Gamlin (2010) showed that, whereas mRGCs and rods contribute significantly to pupil constriction for test stimuli with duration of 100 seconds, cones contribute little (McDougal & Gamlin, 2010) thus indicating that long-duration stimuli could be used to eliminate the intrusion of cones, but retain the contribution of rods.

In the present study, we measured steady-state pupil responses to minimize the intrusion of cones and used very bright stimuli to minimize the intrusion of rods. Furthermore, we used a silent-substitution technique to ensure the isolation of each photoreceptor class. The silent-substitution technique used as selective stimulation of each photoreceptor type is required although selectivity is difficult when spectral sensitivity curves for each photoreceptor overlap. For example, when pupil constriction was measured as a function of the level of light source emission, the pupil constricted as the level of emission increased, indicating that brightness information was conveyed to the midbrain. Under these conditions, pupil constriction can be attributed to amalgamated increases in excitation of the classical photoreceptors and mRGCs (e.g. Berman, 2008; Vienot et al, 2009). Alternatively, a monochromatic light of ~500 nm could be used to stimulate selectively mRGCs but this would stimulate classical photoreceptors and hence subsequently induce the perception of luminance and color. The present study employed a four-primary stimulating system with a silent-substitution technique that allows independent control of the stimulation of the mRGCs in a test stimulus field. The system allows direct measurements of pupillary functions for mRGCs and cones. Excitation of the three types of cones was kept constant during mRGC stimulation; hence there was no change in excitation for each cones type between the control stimulus and test stimuli in the mRGC condition (*i.e.*, “silent substitution”). In the mRGC condition the test and control stimuli were so-called metamers that

have the same tristimulus values but different spectral radiant power distributions, indicating that the color and luminance for these stimuli were the same.

The aim of this study was to investigate how mRGC signals and cone-mediated luminance signals contribute to the steady-state pupil response. We varied independently the excitation of mRGCs and luminance levels and show a significant change in pupil diameter with excitation of mRGCs alone when luminance and color remain constant. Furthermore, the results indicate that mRGC signals contribute ~3-times more to the pupillary control pathway than the cone-mediated luminance signals.

Methods

Apparatus

A personal computer and an interface board (NI-6733, National Instruments, USA) controlled a four-primary illumination system (Fig. 1(a)). The illumination system consisted of an optical diffuser and an integrating sphere which presented a 20° circular test field on the optical diffuser. Dacey et al. showed that the population density of mRGCs increases from the peripheral retina to the fovea and has a peak at 2 mm from the fovea (Dacey et al, 2005). Using a procedure proposed by Dacey et al. (Dacey & Petersen, 1992) we calculated that a test field of 20 degrees visual angle was sufficient to encompass the peak of mRGC distribution.

Four different kinds of light-emitting diodes (LEDs, OptoSupply Ltd, Hong Kong) were used as internal light sources in the integrating sphere and their luminance output was controlled by analogue pulse width modulation (PWM) units by adjusting a duty cycle of pulse train to 1 kHz. The peak wavelengths of the four LEDs were 615 nm, 525 nm, 500 nm and 470 nm, with half-height bandwidths of 20-36 nm. The PWM units were controlled by a sixteen-bit digital/analog

converter (PCI-6733, National Instruments, USA). The head of the observer was held stable by a chin-rest.

Figure 1

Estimation of excitation for photoreceptors

In all experiments test stimuli were represented in a receptor-excitation space that used excitations of three types of cones and mRGC. The receptor-excitation space is a natural extension of cone-excitation space. Cone-excitation space uses three fundamentals which correspond to the excitation of the three kinds of retinal cones (Smith & Pokorny, 1996; Tsujimura et al, 2001; Tsujimura et al, 2007). The fundamentals were designed so that the total amount of excitation of L and M cones was equivalent to the photopic luminous efficiency function $V(\lambda)$. We used a fundamental for S cones with a peak of 1.0 to calculate S cone excitation. The fundamental is proportional to the unit (blue troland) used by Boynton and Kambe (Boynton & Kambe, 1980). In addition to these three cone fundamentals, we used a spectral sensitivity curve for mRGC. These fundamentals were mapped onto four orthogonal axes in receptor-excitation space. Excitation of mRGCs was calculated from an estimated spectral sensitivity curve with a peak of 1.0. We assumed that the S cones and mRGCs do not affect the photopic luminosity function (*i.e.*, luminance) although we used photopic luminance units (cd/m^2). The 10-deg cone fundamentals proposed by Stockman *et al.* (Stockman et al, 1999; Stockman & Sharpe, 2000) were used to calculate the excitation of cones.

We estimated the spectral sensitivity of mRGCs from a pigment template nomogram (Dartnall, 1953) with a peak wavelength, λ_{max} , of 482 nm (Govardovskii et al, 2000). Dacey *et al.* showed

that a spectral tuning curve of mRGCs as a function of wavelength was closely approximated by a pigment template with a peak at 482 nm (Dacey et al, 2005). The lens and macular pigment density spectra employed were those of Stockman *et al* (Stockman et al, 1999), that is, 1.7649 at 400 nm and 0.095 at 460 nm, respectively (CIE, 2006). The fraction of incident light absorbed by the receptor depends on D_{peak} , peak axial optical density. Stockman *et al.* chose values of 0.38 for M and L cones and 0.30 for S cones respectively. The peak axial density for cones is estimated from the length of cone outersegment. Despite limited reference information we estimated 0.5 as the optimum D_{peak} for mRGC. A lower value would be more applicable when the body of melanopsin ganglion cells is shorter than the outersegment of cones. In addition, the D_{peak} influences the shape of the spectral sensitivity curve; for example, when an estimation of D_{peak} is high, a broadening absorption spectrum is likely. However, because we used LEDs with peaks of 500 and 525 nm, which have relatively large half-band widths (33 nm and 36 nm, respectively), it has been assumed that the effect of D_{peak} on spectral sensitivity curve was minimal. The mRGC excitation estimated from a D_{peak} of 0.1 was slightly (0.16 %) smaller than that with a D_{peak} of 0.5 at the maximum contrast of 53 %. The resultant spectral sensitivity function of mRGC in a 10-deg field displayed a peak wavelength of 502 nm.

Procedure

Six visually corrected (with hydrophilic soft lenses) observers (age range 22-25 years, 3 male and 3 female) participated in the experiment. All observers gave written informed consent, and the study was approved by the local research ethics committee. The observers were seated 30 cm in front of the diffuser and binocularly fixated upon a black Maltese cross (95% contrast), which subtended 1.1° and was always present in the center of the diffuser. The cross acted as an accommodative 'lock,' providing a strong closed-loop stimulus to maintain accommodation at a

constant level. Experimental trials started after an initial adaptation period of 5 minutes. Figure 1 (b) illustrates the presentation sequence of test and control stimuli. The test stimulus was presented for 10 minutes following a control stimulus presentation of 5 minutes. The order of presentation for the five test stimuli, each representing different excitation levels, was counter-balanced across 5 sessions according to a Latin-Square design. Over the course of 20 seconds, the test stimulus changed gradually to the control stimulus and *vice versa*, to minimize the effects of an abrupt step change in stimulus. Under the luminance and radiant energy conditions, some observers were aware of the transition between the test and the control stimuli but none could identify the transition under the mRGC condition. The pupillary diameter was recorded for 2 seconds (120 traces) from the observer's right eye; recording was repeated after an interval of 30 seconds. The total number of traces recorded for each test stimulus was 2400 over a 10 minute session. The procedure was repeated for each observer over the same period of time, on different days. For each observer data were averaged over the number of completed sessions; these were 5 or 10 sessions. All statistical analyses were carried out using a validated statistical analysis pack (R Development Core Team, 2008).

LED calibration

The spectral output of each LED was measured with a spectroradiometer (CS-1000A, KonicaMinolta, Japan). The luminance output of each LED was controlled by PWM units. Although PWM is an efficient technique for offering high LED output linearity, small deviations from linearity in luminance were observed. These deviations were probably caused by the thermal effects of LEDs (Watanabe et al, 1992). We used a second-order polynomial fit to take account of the deviations in each LED.

Measurement of pupil size

The pupil of the right eye was imaged using a video camera (Dragonfly, Point Grey Research, Canada) located 0.5 m from the observer and 28° temporal to the visual axis. The video image was fed into a personal computer and analyzed using LabVIEW and IMAQ Vision software (National Instruments) at a frequency of 60 Hz. The pupil was located using thresholding and edge detection techniques, allowing the pupil diameter to be analyzed at a resolution of <0.001 mm (Tsujimura et al, 2001).

Stimuli

The experiment involved three conditions: under the mRGC condition, test stimuli were used to vary just mRGC excitation; under the luminance condition, the luminance of test stimuli alone were varied.; under the energy condition, the radiant energy of the test stimulus was varied with no change in spectral composition, which reduced radiant energy equally at all wavelengths. Under the latter condition, excitation of all photoreceptor classes varied to a similar extent as those under the luminance and the mRGC conditions. Figure 2 (a) represents test stimuli in receptor-excitation space. The bottom axis represents the luminance of test stimuli that correspond to the sum of excitations of long-wavelength sensitive cones (L cones) and middle-wavelength sensitive cones (M cones); the top axis represents the corresponding relative luminance for the control stimulus. The left axis represents mRGC excitation, and the right axis represents mRGC excitation relative to the control stimulus. The filled circles represent the control stimulus that was also used as one of the test stimuli. The five circles parallel to the horizontal axis represent test stimuli used under the luminance condition; the circles parallel to the vertical axis represent those under the mRGC condition and the circles on the diagonal axis represent those under the radiant energy condition. Under the energy condition, excitation of

short-wavelength sensitive cones (S cones) varied in the same way as for luminance and mRGC excitation and has been omitted for simplicity.

Figure 2 (b) shows a schematic diagram of receptor excitation for each condition. Four panels from (i) to (iv) show receptor excitation of the control (i) and test stimuli (ii-iv); these panels correspond to those with the same label in Fig. 2 (a). The dashed boxes represent the receptor excitation of the control stimulus and the solid boxes represent the excitations when the relative excitation decreased by 53% under each condition. Compared to the control condition, differences in pupil diameter could therefore be attributed to the difference in excitation of each receptor class.

The experiment was designed so that the change in receptor-excitation in the energy condition encompasses the change in receptor-excitation for both the mRGC and luminance conditions thus permitting measurement of the relative contribution of mRGCs to all photoreceptor classes (Fig.2 (b)). The change in pupil diameter under the mRGC condition could, in part, be attributable to change under the energy condition thus reflecting a relative contribution of mRGCs to the pupillary pathway compared to the contribution from all photoreceptor classes in the energy condition. Similarly, the change in pupil diameter under the luminance condition could, in part, be attributable to change under the energy condition. Hence, as shown in the following section, the relative contribution of mRGC and cone-mediated luminance signals to all photoreceptor classes could be obtained.

Figure 2

Rod intrusion

The change in pupil diameter could be induced by rod activity rather than by mRGC activity. Several researchers have shown that rods can produce large pupillary responses e.g.(Alpern & Ohba, 1972; Hansen & Fulton, 1986; McDougal & Gamlin, 2010). Further, McDougal & Gamlin have recently shown that mRGCs and rods contribute significantly to pupil constriction for test stimuli with duration of 100 seconds whereas cones contribute little (McDougal & Gamlin, 2010), suggesting that rod activity can influence the pupil even when using a steady background. We used bright stimuli with ~3640 scotopic trolands for the control stimulus and the lowest retinal illuminance used was ~1710 scotopic trolands throughout to eliminate the intrusion of rods. Aguilar and Stiles showed that rod intrusion is likely to diminish progressively above 100 scotopic trolands and to be entirely absent at 2000-5000 scotopic trolands in color-matching tasks (Aguilar & Stiles, 1954) which suggests that rod intrusion was small or negligible in the present experiment. Also, as data presented in the next section show, the contribution of cone-mediated luminance signals is about three times lower than that of the mRGC signals which further suggests little intrusion of rods since it is reasonable to assume that cone signals contribute more than rod signals to the pupillary control pathway under the bright stimulus conditions used in the present experiment.

Results

Figure 3 (a-c) shows, for two observers, typical results for pupil diameters (a) as a function of relative mRGC excitation, (b) as a function of relative luminance and (c) as a function of relative energy. The stimulus value 1.0 corresponds to the test stimulus that is equivalent to the control stimulus. The vertical axis represents average pupil diameter during the test period. Under the

mRGC condition, the slopes of the linear regression line were significantly negative for all six observers (all $p < 0.05$, regression analysis) although the change in pupil diameter was relatively small owing to measurement of steady-state pupil responses (to minimize the intrusion of cone) and use of a very bright stimuli (to minimize the intrusion of rods). The fact that the slope was negative for all observers indicated that pupil diameter decreases as mRGC excitation increases. Notably, we observed a significant decrease in pupil diameter under the mRGC condition, although the color and luminance of test stimuli were constant. Under the luminance condition, although the slopes for all six observers were negative no significant difference in slope was found for any observer (all, $p > 0.063$, regression analysis). Under the energy condition, the slopes of the linear regression line were significantly negative for all observers (all, $p < 0.05$, regression analysis), indicating that pupil diameter decreases as the radiant energy increases.

Figure 3

When the slope was compared across conditions, it was consistently found that the slopes under the energy condition were significantly greater than those under the mRGC and luminance conditions for all observers ($p = 0.014$ and 0.002 , paired t-test). Moreover, the slopes under the mRGC condition were significantly greater than those under the luminance condition for all observers ($p = 0.010$, paired t-test). These results indicate that mRGC signals contribute more to the pupillary control pathway than the luminance signals. The change in pupil diameter was greatest under the energy condition probably because both the mRGC and the luminance signals contribute to the pupillary control mechanism (Fig.2 (b)).

Because pupil diameter under the control condition differed between observers, measurements for each condition were subtracted from that for the respective control stimulus so that change in pupil diameter from baseline could be determined. The change in pupil diameter for all observers is shown (Fig.4 (a-c)). The left panel shows the change in pupil diameter under the mRGC condition, the middle panel shows the change under the luminance condition, and the right panel shows the change under the energy condition. The slopes of the linear regression line calculated from the averaged change in pupil diameter were significantly negative for all three conditions ($p=0.001$, 0.012 and 0.021 , regression analysis). It was found that the change in pupil diameter for the mRGC condition was about 3 times larger than that for the luminance condition and that the change in diameter under the energy condition was the largest (about 1.5 times larger than that for the mRGC).

Figure 4

The experiment was designed so that the change in receptor-excitation in the radiant energy condition included concomitant changes in receptor-excitation for both the mRGC and luminance conditions (Fig.2(b)). The change in pupil diameter under the energy condition might, therefore, include the change induced by the mRGC condition, and thus reflect a relative contribution of mRGCs to the pupillary pathway compared to the contribution from all photoreceptor classes in the energy condition. Similarly, the change in pupil diameter under the energy condition might, therefore, include the change induced by the luminance condition. Hence, a relative contribution of mRGCs to all photoreceptor classes could be estimated. Figure 4 (d) shows the relative contribution of mRGC and cone-mediated luminance signals to all

photoreceptor classes. The relative contribution was calculated from the respective changes in pupil diameter for mRGC and luminance conditions indicated in Fig.4 (a,b) divided by those for the energy condition in Fig.4 (c). The horizontal axis represents the receptor excitation under the mRGC and luminance conditions relative to the control stimulus. As the stimulus with relative excitation 1.0 was equivalent to the control stimulus under all conditions, it was excluded from the Figure. The vertical axis represents the relative contribution of mRGC and luminance signals to all receptor classes. The relative contribution of mRGC is clearly larger than that for luminance at all relative levels of receptor excitation. The relative contribution of mRGC increases monotonically and exceeds 1.0, indicating that the change in pupil diameter under the mRGC condition was slightly greater than that under the energy condition at the highest excitation level (see also Fig.4 (a, c)). These results demonstrate that mRGC signals, which were about triple the strength of the cone-mediated luminance signals, contribute substantially to the steady-state pupillary control pathway at higher excitation levels.

Discussion

Contribution of mRGC and cone signals to the pupillary control pathway

We found that the relative change in pupil diameter for the mRGC condition was ~3 times larger than that for the luminance condition, that is, mRGCs contribute 3 times more than L and M cones as luminance signals were defined as a sum of L- and M-cone excitations. The results are consistent with those of a previous study that used transgenic animals. Lucas *et al.* generated transgenic mice lacking melanopsin and mice lacking the classical photoreceptors. Thus, each phenotype was complementary in function. Lucas *et al.* measured pupil diameter as a function of irradiance and found that the melanopsin-associated signals contribute more to the pupillary control pathway than signals from the classical photoreceptors at high irradiances (>12 log

photons/cm²/sec) (Lucas et al, 2003). Because we chose the control stimulus to have an irradiance of 13.7 log photons/cm²/sec, the mRGC signals in humans also contribute more to the pupillary control pathway than L- and M-cone signals.

The question arises as to how mRGC and cone signals are summed and contribute to the pupillary control pathway. Lucas *et al.* showed that the irradiance-response function in wild-type mice can be predicted from a simple sum of functions derived respectively from mice lacking the classical photoreceptors and mice lacking melanopsin (Lucas et al, 2003). In the present experiment the results in Fig.4 (a-c) indicate that the slope under the energy condition was more than the simple summation of slopes under the mRGC and luminance conditions, that is, the change in pupil diameter in the energy condition was more than the simple summation of those in mRGC and the luminance conditions. Furthermore, the results in Fig.4 (d) showed that the simple summation of changes for the mRGC and luminance conditions was more than 1.0 at higher excitation levels (i.e. >1.265), suggesting that there could be a subtractive or inhibitory combination of the mRGC and luminance signals. Conversely, at the relative receptor excitation of 0.47, the linear summation of mRGC and luminance was significantly less than 1.0, suggesting a non-linear additive combination of mRGC and luminance signals. It seems reasonable to conclude that in humans the mRGC signals contribute approximately three times more to the steady-state pupil responses compared to the cone-mediated luminance signals. How mRGC and cone signals are non-linearly summed is a matter for future research.

Effect of bistability

Mure et al. proposed a model in which there is a bistable state with different absorbance spectra for melanopsin: the R absorption spectrum has a peak wavelength of 481 nm and the M absorption spectrum has a peak wavelength of 587 nm (Mure et al, 2009). Since the silent-

substitution technique used in the present experiment depends on the spectral sensitivity curve for each photoreceptor, the presence of bistability could influence the results. Although the data did not show either the absence or existence of melanopsin bistability the potential effect on the results is considered to be small. Since one session in the experiment had a duration of 85 minutes (see Fig.1 (b)) it is possible that bistability could influence the results during the course of a single session. The pupil diameter in the control stimulus condition (presented at ten-minute intervals) would vary according to the transition of the peaks but no systematic changes in pupil size were evident indicating that the effect of bistability is likely to be small or negligible. Moreover, the effect of bistability, albeit small, is likely to be counter-balanced across conditions by the Latin Square design of the presentation sequence.

This paper is dedicated to the memory of our friend and co-author, Kazuhiko Ukai, who made a significant contribution to this project before he passed away on November 1st, 2009.

This work is partially supported by the Japanese Ministry of Education, Science, Sports and Culture, Grant-in-Aid for Scientific Research (C), 21570247 (2009-2011) to Sei-ichi Tsujimura, and also by the Great Britain Sasakawa Foundation Butterfield Awards for UK-Japan collaboration in medical research and public health practice. We thank Bernard Gilmartin for reading the entire manuscript and making a number of helpful comments.

FIGURE CAPTIONS

Figure 1

(a) Set-up for the experiments. A personal computer and an interface board controlled a four-primary illumination system. The illumination system consisted of an optical diffuser and an integrating sphere which presented a 20° circular field onto the optical diffuser. The luminance output of each LED was controlled by analogue pulse width modulation (PWM) units by adjusting a duty cycle of pulse train. (b) An example of a presentation sequence of test and control stimuli used in the experiment; test stimuli with 5 different excitation levels were used. The order of presentation for the five test stimuli was counter-balanced across 5 sessions according to a Latin-Square design.

Figure 2

(a) Test stimuli represented in a receptor-excitation space. The bottom axis represents the luminance for test stimuli and the top axis represents the corresponding relative luminance. The left axis represents mRGC excitation and the right axis represents relative mRGC excitation. The filled circles represent the control stimulus. The control stimulus had CIE coordinates (0.58, 0.36) and a luminance of 642 cd/m². The receptor excitations for the control stimulus were 506 cd/m² for the L cone, 136 cd/m² for the M cone, 46 cd/m² for the S cone and 192 cd/m² for the mRGC (see Methods for details). The retinal irradiance in photon flux of the control stimulus was 13.7 log photons/cm²/sec. The circles parallel to the horizontal axis represent the five test stimuli used under the luminance condition; the circles parallel to the vertical axis represent those used under the mRGC condition; the circles on the diagonal axis represent those used under the energy condition. (b) The photoreceptor excitations for the control (dashed line) and

the test stimuli (solid line) with the relative excitation of -53% compared with the control stimulus. The labels from (a) to (d) correspond to the specific test stimuli indicated in Fig 2(a).

Figure 3

Typical results for pupil diameters (a) as a function of relative mRGC excitation, (b) as a function of relative luminance and (c) as a function of relative energy for two observers. The horizontal axis represents relative excitation and the vertical axis represents average pupil diameter. The dashed line indicates the regression line. The values of the slopes of the regression line are provided in the upper right of the panel and the 95% confidence limits for the slope are given in brackets. Error bars indicate 1 s.e.m. (n=5).

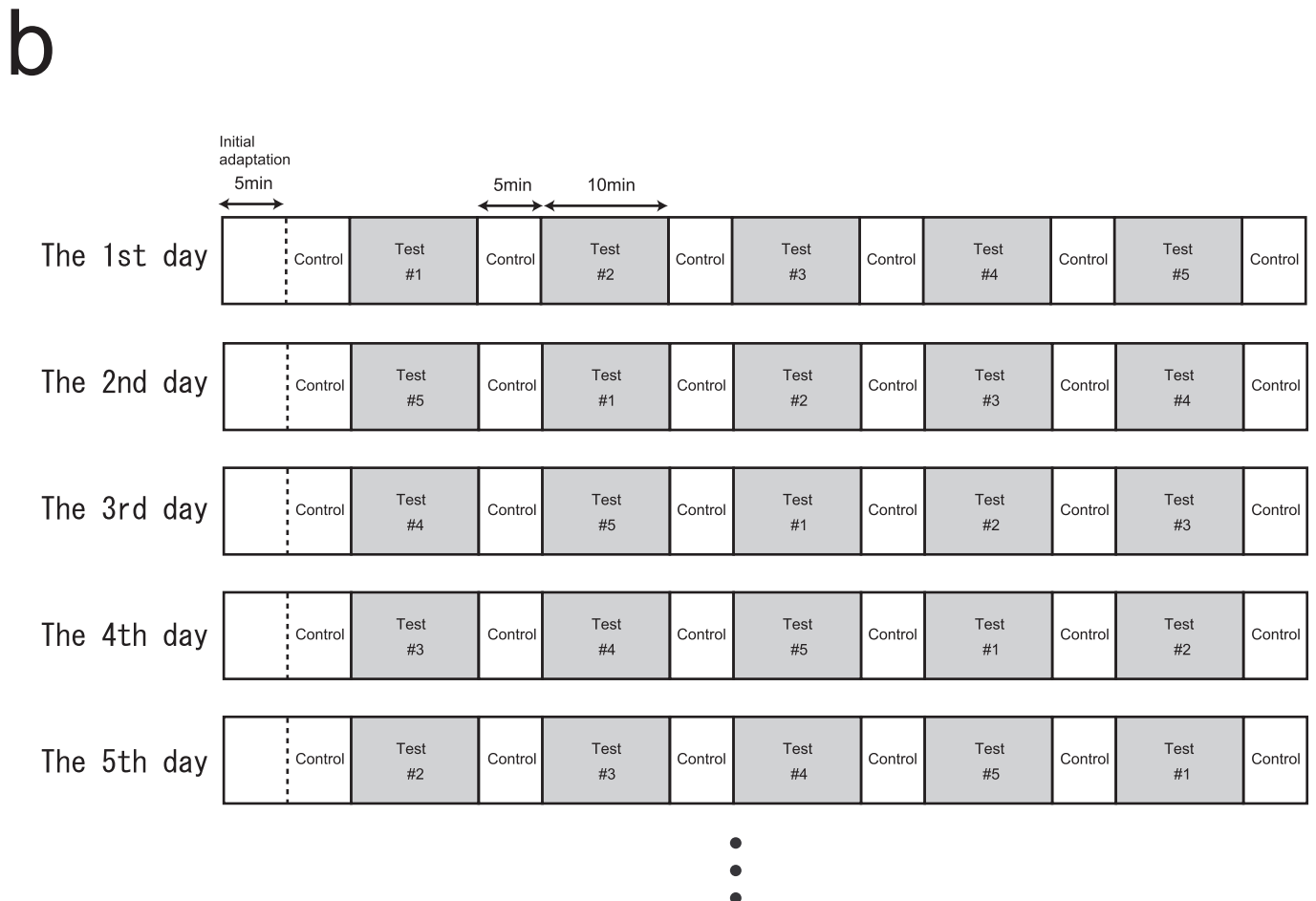
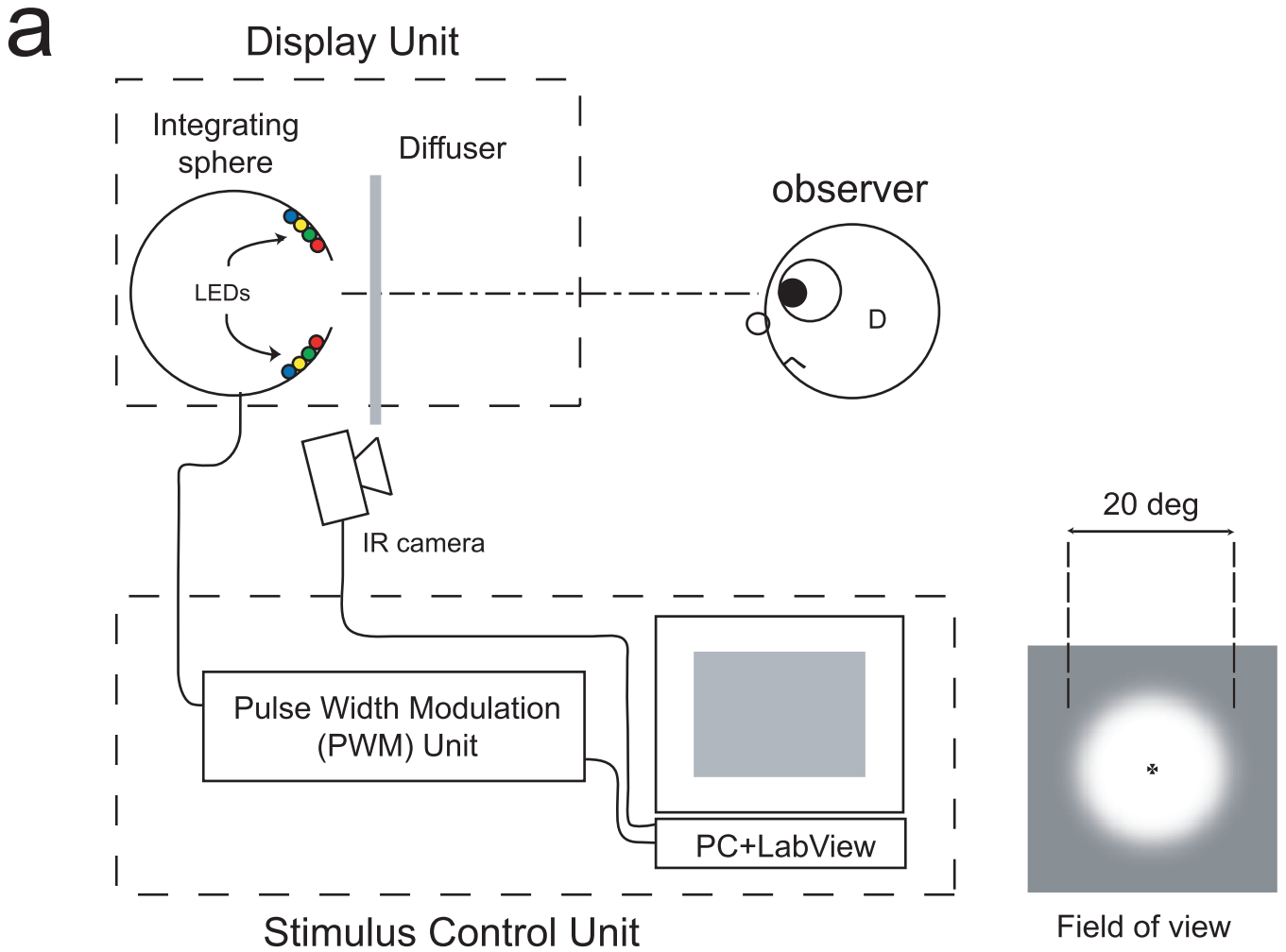
Figure 4

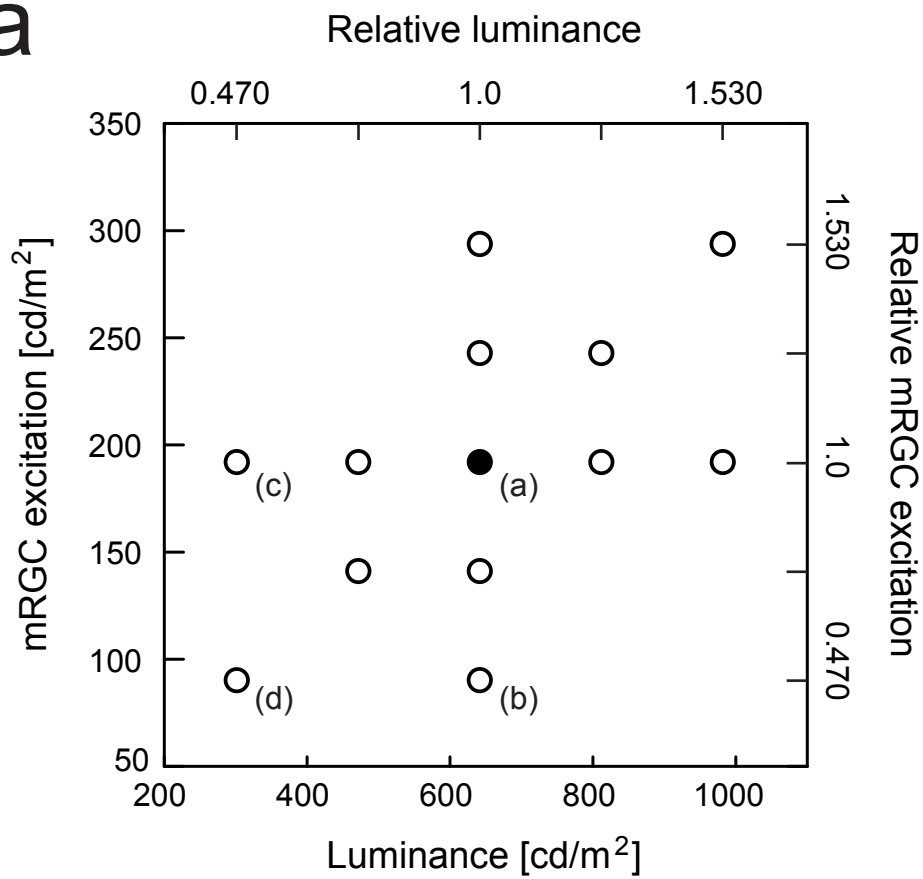
Change in pupil diameter for all observers (a) under the mRGC condition, (b) under the luminance condition and (c) under the energy condition. The horizontal axis represents relative excitation and the vertical axis represents change in pupil diameter for all observers. The dashed line shows the regression line averaged across all observers. The values of the slopes of the regression line are provided in the upper right in the panel and the 95% confidence limits for the slope are given in brackets. (d) The relative contribution of mRGC and L+M luminance signals to all photoreceptor classes at each relative receptor excitation. The change in pupil diameter under the mRGC and luminance conditions (Fig 4a,b) normalized with respect to the change under the energy condition (Fig 4c).

REFERENCES

- Aguilar, M. & Stiles, W.S. 1954 Saturation of the rod mechanism of the retina at high levels of stimulation. *Journal Of Modern Optics*. Taylor & Francis, 1, 59-65.
- Alpern, M. & Ohba, N. 1972 The effect of bleaching and backgrounds on pupil size. *Vision Res.*, 12, 943-951.
- Berman, S.M. 2008 A new retinal photoreceptor should affect lighting practice *Light Res. Technol.*, 40, 373-376.
- Boynton, R.M. & Kambe, N. 1980 Chromatic difference steps of moderate size measured along theoretically critical axes. *Color Res. Appl.*, 5, 13-23.
- C.I.E. 2006 Fundamental Chromaticity Diagram with Physiological Axes - Part 1 Publ. CIE. No. 170-1. Bureau. Central. de. la. SIE,, , Paris.
- Dacey, D.M. & Petersen, M.R. 1992 Dendritic field size and morphology of midget and parasol ganglion cells of the human retina. *Proc. Natl. Acad. Sci. U. S. A.*, 89, 9666-9670.
- Dacey, D.M., Liao, H.W., Peterson, B.B., Robinson, F.R., Smith, V.C., Pokorny, J., Yau, K.W. & Gamlin, P.D. 2005 Melanopsin-expressing ganglion cells in primate retina signal colour and irradiance and project to the LGN. *Nature*, 433, 749-754.
- Dartnall, H.J. 1953 The interpretation of spectral sensitivity curves. *Br. Med. Bull.*, 9, 24-30.
- Gamlin, P.D., McDougal, D.H., Pokorny, J., Smith, V.C., Yau, K.W. & Dacey, D.M. 2007 Human and macaque pupil responses driven by melanopsin-containing retinal ganglion cells. *Vision Res.*, 47, 946-954.
- Govardovskii, V.I., Fyhrquist, N., Reuter, T., Kuzmin, D.G. & Donner, K. 2000 In search of the visual pigment template. *Vis. Neurosci.*, 17, 509-528.
- Hansen, R.M. & Fulton, A.B. 1986 Pupillary changes during dark adaptation in human infants. *Invest. Ophthalmol. Vis. Sci.*, 27, 1726-1729.
- Hattar, S., Lucas, R.J., Mrosovsky, N., Thompson, S., Douglas, R.H., Hankins, M.W., Lem, J., Biel, M., Hofmann, F., Foster, R.G. & Yau, K.W. 2003 Melanopsin and rod-cone photoreceptive systems account for all major accessory visual functions in mice. *Nature*, 424, 76-81.
- Kardon, R., Anderson, S.C., Damarjian, T.G., Grace, E.M., Stone, E. & Kawasaki, A. 2009 Chromatic pupil responses: preferential activation of the melanopsin-mediated versus outer photoreceptor-mediated pupil light reflex. *Ophthalmology*, 116, 1564-1573.
- Lucas, R.J., Douglas, R.H. & Foster, R.G. 2001 Characterization of an ocular photopigment capable of driving pupillary constriction in mice. *Nat. Neurosci.*, 4, 621-626.
- Lucas, R.J., Hattar, S., Takao, M., Berson, D.M., Foster, R.G. & Yau, K.W. 2003 Diminished pupillary light reflex at high irradiances in melanopsin-knockout mice. *Science*, 299, 245-247.
- McDougal, D.H. & Gamlin, P.D. 2010 The influence of intrinsically-photosensitive retinal ganglion cells on the spectral sensitivity and response dynamics of the human pupillary light reflex. *Vision Res.*, 50, 72-87.
- Mrosovsky, N. & Hattar, S. 2003 Impaired Masking Responses to Light in Melanopsin-Knockout Mice. *Chronobiology International*, 20, 989-999.
- Mure, L.S., Cornut, P.L., Rieux, C., Drouyer, E., Denis, P., Gronfier, C. & Cooper, H.M. 2009 Melanopsin bistability: a fly's eye technology in the human retina. *PLoS. One.*, 4, e5991.
- Panda, S., Sato, T.K., Castrucci, A.M., Rollag, M.D., DeGrip, W.J., Hogenesch, J.B., Provencio,

- I. & Kay, S.A. 2002 Melanopsin (Opn4) requirement for normal light-induced circadian phase shifting. *Science*, 298, 2213-2216.
- Panda, S., Provencio, I., Tu, D.C., Pires, S.S., Rollag, M.D., Castrucci, A.M., Pletcher, M.T., Sato, T.K., Wiltshire, T., Andahazy, M., Kay, S.A., Van Gelder, R.N. & Hogenesch, J.B. 2003 Melanopsin is required for non-image-forming photic responses in blind mice. *Science*, 301, 525-527.
- R Development Core Team 2005 R: A language and environment for statistical computing. R Foundation for Statistical Computing, Vienna, Austria. ISBN 3-900051-07-0, URL <http://www.R-project.org>. "
- Ruby, N.F., Brennan, T.J., Xie, X., Cao, V., Franken, P., Heller, H.C. & O'Hara, B.F. 2002 Role of melanopsin in circadian responses to light. *Science*, 298, 2211-2213.
- Smith, V.C. & Pokorny, J. 1996 The design and use of a cone chromaticity space: A tutorial. *Color Res. Appl.*, 21, 375-383.
- Stockman, A., Sharpe, L.T. & Fach, C. 1999 The spectral sensitivity of the human short-wavelength sensitive cones derived from thresholds and color matches. *Vision Res.*, 39, 2901-2927.
- Stockman, A. & Sharpe, L.T. 2000 The spectral sensitivities of the middle- and long-wavelength-sensitive cones derived from measurements in observers of known genotype. *Vision Res.*, 40, 1711-1737.
- Tsujimura, S., Wolffsohn, J.S. & Gilmartin, B. 2001 A linear chromatic mechanism drives the pupillary response. *Proc. Biol. Sci.*, 268, 2203-2209.
- Tsujimura, S., Shioiri, S. & Nuruki, A. 2007 Two distinct cone-opponent processes in the L+ M luminance pathway. *Vision Res.*, 47, 1839-1854.
- Vienot, F., Durand, M.L. & Mahler, E. 2009 Kruithof's rule revisited using LED illumination *J. Mod. Optic.*, 56, 1433-1446.
- Watanabe, T., Mori, N. & Nakamura, F. 1992 A new superbright LED stimulator: photodiode-feedback design for linearizing and stabilizing emitted light. *Vision Res.*, 32, 953-961.
- Young, R.S. & Kimura, E. 2008 Pupillary correlates of light-evoked melanopsin activity in humans. *Vision Res.*, 48, 862-871.
- Zaidi, F.H., Hull, J.T., Peirson, S.N., Wulff, K., Aeschbach, D., Gooley, J.J., Brainard, G.C., Gregory-Evans, K., Rizzo, J.F. 3rd, Czeisler, C.A., Foster, R.G., Moseley, M.J. & Lockley, S.W. 2007 Short-wavelength light sensitivity of circadian, pupillary, and visual awareness in humans lacking an outer retina. *Curr. Biol.*, 17, 2122-2128.



a**b**